

Analyzing Sulfur-doped Li_3InCl_6 Solid Electrolytes by X-ray Absorption Spectroscopy

Mariya Yamagishi¹, Shintaro Tachibana¹, Takeshi Shimizu¹, Kei Mitsuhara²,
and Yuki Orikasa¹

- 1) *Department of Applied Chemistry, Graduate School of Life Sciences, Ritsumeikan University, 1-1-1 Noji-Higashi, Kusatsu 525-8577, Japan*
- 2) *Ritsumeikan Global Innovation Research Organization, Ritsumeikan University, 1-1-1 Noji-Higashi, Kusatsu, Shiga 525-8577, Japan*

Solid electrolytes are key materials for improving the performance of all-solid-state rechargeable batteries, which are required to be highly ionically conductive, chemically stable, and formable. Despite a large number of studies on single-anion sulfide- or oxide-based solid electrolytes, there have been no reports on the synthesis of anion-doped chloride-based solid electrolytes. In this study, we doped the Li_3InCl_6 lithium-ion conductor with highly polarizable sulfide ions. The synthesized samples were characterized by X-ray diffraction and Cl K -edge and In L_3 -edge X-ray absorption spectroscopy. Sulfide-ion doping was found to perturb the electronic structure of the Cl 3p orbital and the local structure around In, while maintaining the crystal structure of Li_3InCl_6 .

1. Introduction

Lithium-ion batteries that use flammable organic electrolytes suffer from safety issues. In order to improve safety, all-solid-state batteries that use non-flammable inorganic solid electrolytes are being continually developed. In general, all-solid-state batteries are safer and more reliable than lithium-ion batteries, and are expected to charge at high rates because the transport number of a solid electrolyte is almost unity^{1, 2}. Although studies into solid electrolytes have mainly focused on oxides and sulfides³, halide-based materials are also promising because of their high lithium-ion conductivities^{4, 5}, which is expected based on the properties of halide ions. Lithium ions are expected to be highly diffusive in such materials because monovalent halides interact more weakly with lithium ions compared to divalent sulfur or oxygen anions. Li_3YCl_6 , Li_3YBr_6 , and Li_3InCl_6 , which exhibit lithium-ion conductivities of $10^{-3} \text{ S cm}^{-1}$ at room temperature, have been reported to be halide-based solid electrolytes^{4, 5}. Most of these compounds are single-anion chlorides, with lithium-ion conductors based on multiply anionic chlorides not reported to date. Recently, material science studies into mixed-anion compounds have expanded⁶ and such compounds have recently been reported as battery materials⁷. In this study, we prepared a mixed-anion Li_3InCl_6 /sulfur solid electrolyte using a solid-state reaction. The prepared Li_3InCl_6 and $\text{Li}_3\text{InCl}_{5.4}\text{S}_{0.6}$ were characterized by X-ray diffraction (XRD), and X-ray absorption spectroscopy (XAS), which have been used to analyze mixed-anion fluorides^{8, 9}. We show that XAS is an effective method for verifying that the chloride-based solid electrolyte is anion-doped.

2. Experimental

Li_3InCl_6 was prepared by mixing LiCl and InCl₃ in a 3:1 molar ratio in a mortar in an Ar-filled glove box, while $\text{Li}_3\text{InCl}_{5.4}\text{S}_{0.6}$ was prepared from LiCl, InCl₃, In₂S₃, and S in a 30:8:1:3 molar ratio. The mixtures

were milled in a planetary ball mill (Fritsch, P-7) with zirconia balls at 600 rpm for 20 h. The milled powders were then calcined at 260 °C for 5 h under Ar. The XRD experiment was performed using an Ultima-IV diffractometer (Rigaku) with Cu K α radiation as the X-ray source and a tube voltage and current of 40 kV and 40 mA, respectively. These experiments were performed without exposure to air. The XAS experiments at Cl K -edge and In L_3 -edge were carried out at the BL-13 beamline of the Ritsumeikan University SR Center. The powder sample was placed on carbon tape, and the spectra were taken in total electron yield mode under vacuum. Theoretical calculations of the X-ray absorption near edge structure (XANES) at the Cl K -edge of Li_3InCl_6 were performed using the CASTEP pseudopotential density functional theory (DFT) code with the generalized gradient approximation approach of Perdew–Burke–Ernzerhof (GGA-PBE). Geometries were optimized using the BFGS method to meet the convergence criterion of $2.0 \times 10^{-6} \text{ eV/atom}$ for SCF tolerance. A pulse density mixing scheme was used for self-consistent-field calculations. XANES calculations were performed using a core-hole treatment that involved removing the charge of the 1s electron from the absorbed atom while smearing a neutralizing charge over the entire system. Theoretical calculations were also carried out for KCl as a reference.

3. Results and Discussion

We first examined the change in the crystal structure of Li_3InCl_6 when doped with sulfur anions; Figure 1 shows XRD patterns of the synthesized Li_3InCl_6 and $\text{Li}_3\text{InCl}_{5.4}\text{S}_{0.6}$. Most of the observed peaks are indexed to the monoclinic $C2/m$ space group and are consistent with the reported powder diffraction file (PDF) for Li_3InCl_6 (ICDD: 01-070-3274). The unindexed diffraction peaks in the 20–30° 2 θ range are derived from the plastic sample cover. The calculated lattice parameters for Li_3InCl_6 , namely: $a = 6.425 \pm 0.005 \text{ \AA}$,

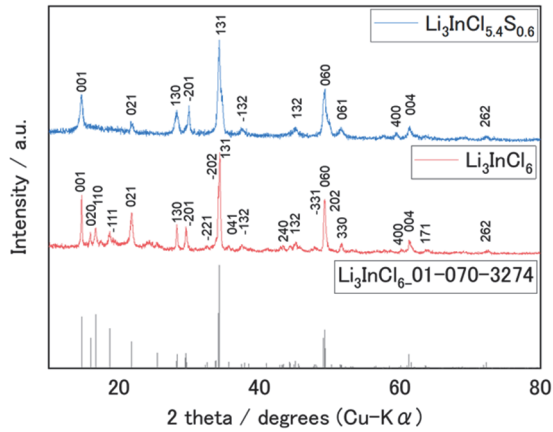


Fig. 1 XRD patterns of the synthesized Li_3InCl_6 and $\text{Li}_3\text{InCl}_{5.4}\text{S}_{0.6}$, and the Li_3InCl_6 reference (ICDD : 01-070-3274).

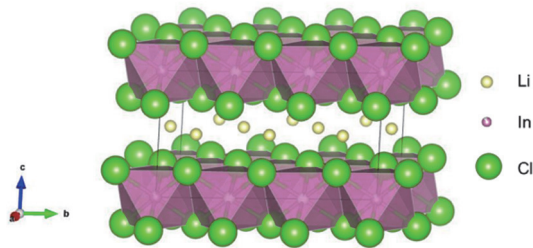


Fig. 2 Crystal structure of Li_3InCl_6 .

$b = 11.091 \pm 0.005$ Å, $c = 6.407 \pm 0.005$ Å, and $\beta = 109.84 \pm 0.07^\circ$, are close to the literature values¹⁰. These results indicate that single-phase Li_3InCl_6 was obtained in this study. A comparison of the XRD patterns of Li_3InCl_6 and $\text{Li}_3\text{InCl}_{5.4}\text{S}_{0.6}$ reveals that the crystal structure of Li_3InCl_6 is retained upon sulfur-anion doping, with no impurity peaks observed; however, the peaks are broader and some peaks are split, which are considered to be due to lower crystallinity and symmetry. The calculated lattice parameters of $\text{Li}_3\text{InCl}_{5.4}\text{S}_{0.6}$ are: $a = 6.44 \pm 0.02$ Å, $b = 11.11 \pm 0.04$ Å, $c = 6.37 \pm 0.04$ Å, and $\beta = 109.9 \pm 0.3^\circ$. When compared with the lattice parameters of the Li_3InCl_6 sample, the sulfur-doped sample is smaller in the c-axis direction, with a large change in the a-axis direction also observed. The ionic radius of sulfur (184 pm) is larger than that of chlorine (181 pm)¹¹, which explains why the cell volume expands when the Cl sites are substituted by S. Figure 2 shows the crystal structure of Li_3InCl_6 . The anion sublattice has a cubic close packing (CCP) configuration, with the trivalent indium cations producing two cation vacancies per indium to form octahedral sites, each with a 3:1:2 Li^+ -to- In^{3+} -to-vacancy ratio. We assume that the electronic states and local structures of Cl and In are altered due to S-anion doping at Cl sites.

We examined the XANES spectra of KCl, as a

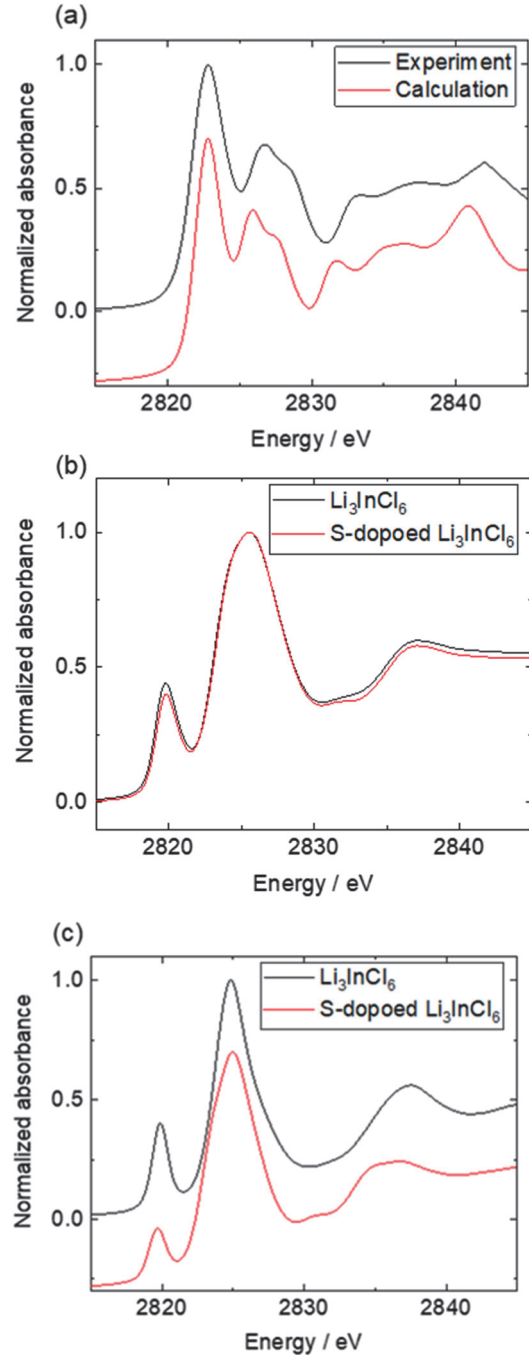


Fig. 3 (a) Comparing the experimental and calculated Cl K -edge XANES spectra of KCl. (b) Cl K -edge XANES spectra of Li_3InCl_6 and $\text{Li}_3\text{InCl}_{5.4}\text{S}_{0.6}$. (c) Calculated XANES spectra of Li_3InCl_6 and S-doped Li_3InCl_6 .

standard, to verify that the experimental and calculated Cl K -edge XANES spectra are consistent. As shown in Fig. 3(a), the calculated spectrum is very similar to the experimentally determined one, which validates the theoretical approach used in this study.

Sulfur-anion doping changes the electronic structure of the Cl 3p orbital. Figure 3(b) shows Cl K -

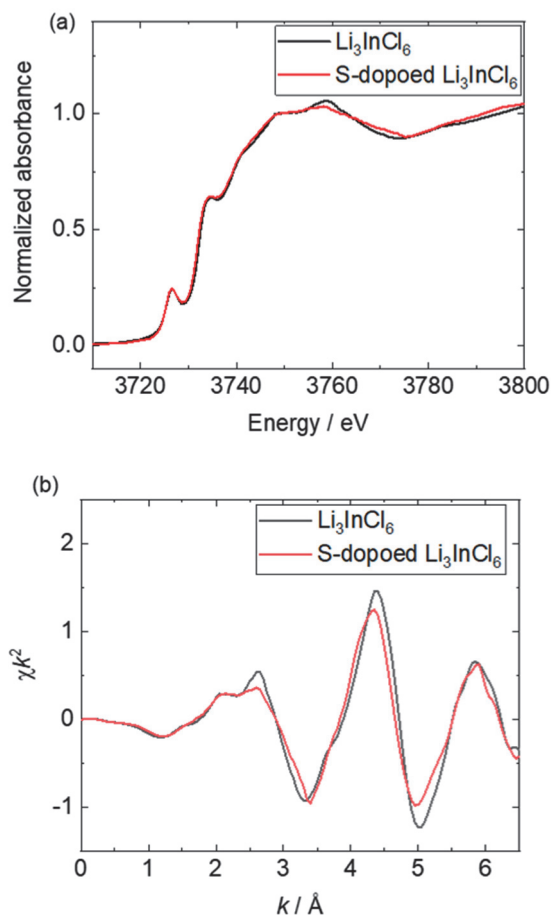


Fig. 4 (a) In L_3 -edge XANES spectra of Li_3InCl_6 and $\text{Li}_3\text{InCl}_{5.4}\text{S}_{0.6}$. (b) EXAFS oscillation, $k\chi^2$ at the In L_3 -edge of Li_3InCl_6 and $\text{Li}_3\text{InCl}_{5.4}\text{S}_{0.6}$.

edge XANES spectra of Li_3InCl_6 and $\text{Li}_3\text{InCl}_{5.4}\text{S}_{0.6}$. Because the spectrum corresponds to the excitation of chlorine from its 1s orbital to the outermost empty 3p orbital, the structure is influenced by changes in chemical bonding through sulfur doping. A pre-edge peak is observed at 2820 eV from the low-energy side, with a main peak observed at approximately 2825 eV. While the spectra of the two samples exhibit no differences in the energies of these two peaks, there are clear differences in peak intensity. Sulfur doping resulted in a less intense pre-edge peak and a more intense main peak. These results were compared with those obtained using theoretical calculations. Figure 3(c) shows the theoretically calculated Cl K -edge spectra of Li_3InCl_6 and $\text{Li}_3\text{In}_{1.125}\text{Cl}_{5.625}\text{S}_{0.375}$. The settings for the crystal structure of the S-doped composition are different from the experimental composition due to the size of the super cell and the electrical neutrality. When normalized against the intensity of the main peak, these calculations confirm that the pre-edge peak is less intense in the S-doped sample. Because the crystal structure is retained during

S-doping and the less-intense pre-edge peak observed in the experimental spectrum is consistent with the theoretically calculated spectrum, we conclude that the Cl sites in Li_3InCl_6 were successfully doped with S in this study. The calculated XANES of the S-doped Li_3InCl_6 shows a significantly weaker pre-edge peak compared with the experimental spectrum. At this moment, we do not have a clear explanation for this difference, but speculate that either 10% S-doping is not sufficiently caused, or that the theoretical calculations cannot accurately reproduce differences in trace doping. The difference in S doping has a major effect on the local structure around In. Figure 4(a) shows the In L_3 -edge XANES spectra of Li_3InCl_6 and $\text{Li}_3\text{InCl}_{5.4}\text{S}_{0.6}$, which correspond to the 2p \rightarrow 4d orbital transitions of indium. No significant change was observed in the spectrum following S-doping, indicating negligible electronic structure change in the In 4d unoccupied orbital. On the other hand, because In is octahedrally coordinated to Cl, S doping significantly distorts the local structure around In. Figure 4(b) shows extended X-ray absorption fine structure oscillations at the In L_3 -edge, which shows that Li_3InCl_6 exhibits larger amplitudes than $\text{Li}_3\text{InCl}_{5.4}\text{S}_{0.6}$ and reflects the distorted local structure around In through the substitution of S at the Cl sites of InCl_6 octahedra.

4. Conclusion

We doped sulfur anions at the anionic sites of the chloride-based Li_3InCl_6 solid electrolyte. XRD revealed that the Li_3InCl_6 lattice expands without the formation of any impurity phase and crystal-structure transition. Cl K -edge XANES revealed that sulfur doping leads to less-intense pre-edge peaks, which is supported by theoretically calculated spectra. In contrast, In L_3 -edge XANES did not show any clear differences due to S-doping, while the EXAFS oscillations were less intense due to S-doping, consistent with a distorted local structure around In. XAS is an effective method for verifying that chloride-based solid electrolytes are anion-doped. This study revealed that anion doping of chloride-based solid electrolytes results in electronic and local structural changes; these chemical changes are useful for improving ionic conductivity as well as potential and chemical stabilities.

References

- [1] H. Buschmann, J. Dolle, S. Berendts, A. Kuhn, P. Bottke, M. Wilkening, P. Heitjans, A. Senyshyn, H. Ehrenberg, A. Lotnyk, V. Duppel, L. Kienle and J. Janek, *Phys. Chem. Chem. Phys.*, **2011**, 13, 19378.
- [2] K. Minami, F. Mizuno, A. Hayashi and M. Tatsumisago, *Solid State Ionics*, **2007**, 178, 837.
- [3] N. Kamaya, K. Homma, Y. Yamakawa, M. Hirayama, R. Kanno, M. Yonemura, T. Kamiyama, Y.

- Kato, S. Hama, K. Kawamoto and A. Mitsui, *Nature Mater.*, **2011**, *10*, 682.
- [4] T. Asano, A. Sakai, S. Ouchi, M. Sakaida, A. Miyazaki and S. Hasegawa, *Adv. Mater.*, **2018**, *30*, 1803075.
- [5] X. Li, J. Liang, J. Luo, M. Norouzi Banis, C. Wang, W. Li, S. Deng, C. Yu, F. Zhao, Y. Hu, T.-K. Sham, L. Zhang, S. Zhao, S. Lu, H. Huang, R. Li, K. R. Adair and X. Sun, *Energy Environ. Sci.*, **2019**, *12*, 2665.
- [6] H. Kageyama, K. Hayashi, K. Maeda, J. P. Attfield, Z. Hiroi, J. M. Rondinelli and K. R. Poeppelmeier, *Nature Comm.*, **2018**, *9*, 772.
- [7] S. Tachibana, K. Ide, T. Tojigamori, Y. Yamamoto, H. Miki, H. Yamasaki, Y. Kotani and Y. Orikasa, *Chem. Lett.*, **2021**, *50*, 120.
- [8] S. Tachibana, T. Ohta and Y. Orikasa, *Mem. SR Center Ritsumeikan Univ.*, **2019**, *21*, 7.
- [9] T. Tsukamoto, S. Tachibana and Y. Orikasa, *Mem. SR Center Ritsumeikan Univ.*, **2020**, *22*, 3.
- [10] M. O. Schmidt, M. S. Wickleder and G. Meyer, *Z. Anorg. Allg. Chem.*, **1999**, *625*, 539.
- [11] R. D. Shannon, *Acta Crystallogr. Sect. A*, **1976**, *32*, 751.